How are GICs and ionospheric currents critical for understanding energy coupling in the ITM system?

Dr. Gareth W. Perry
Center for Solar-Terrestrial Research

March 16, 2022

Solar and Space Physics Decadal Survey White Papers Workshops

The Future of Ground-Based Research for Magnetospheric and ITM Physics (Virtual)

Panel 4

- Measurements of field aligned currents allow us to specify energetic input from the magnetosphere into the ionosphere-thermosphere system.
- By combining FAC and electric field measurements, we can compute an estimate of electromagnetic energy dissipated into the IT system:

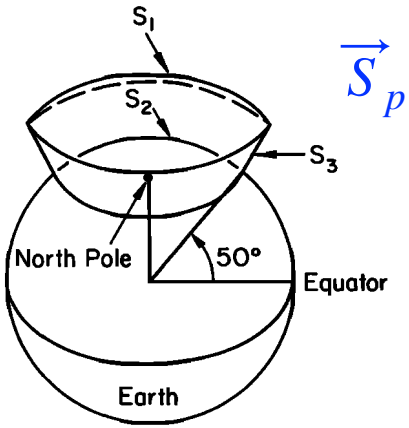

$$\vec{S}_p = \frac{1}{\mu_0}\vec{E} \times \delta\vec{B}$$

Kelley, M. C., Knudsen, D. J., & Vickrey, J. F. (1991). Poynting flux measurements on a satellite: A diagnostic tool for space research. *Journal of Geophysical Research*, *96*(A1), 201. https://doi.org/10.1029/90JA01837

Richmond, A. D. (2010). On the ionospheric application of Poynting's theorem. *Journal of Geophysical Research*, *115*(A10), A10311. https://doi.org/10.1029/2010JA015768

DMSP

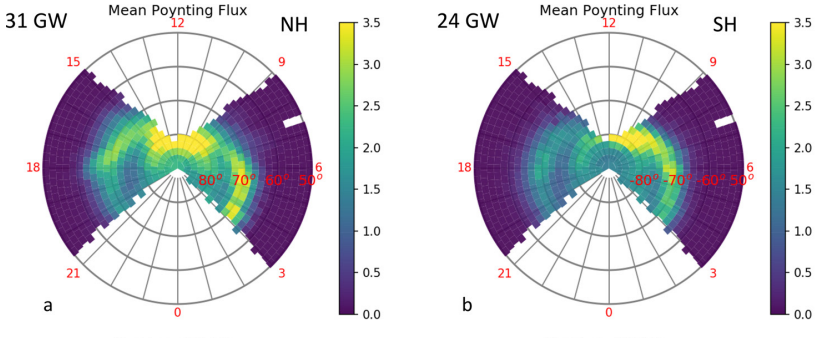

Knipp, D., Kilcommons, L., Hairston, M., & Coley, W. R. (2021). Hemispheric Asymmetries in Poynting Flux Derived From DMSP Spacecraft. Geophysical Research Letters, 48(17), 1–11. https://doi.org/10.1029/2021GL094781

SuperDARN + AMPERE

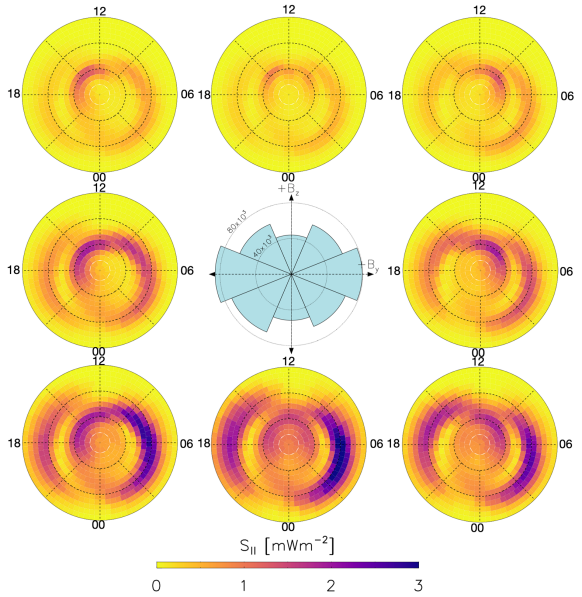

Billett, D. D., Perry, G. W., Clausen, L. B. N., Archer, W. E., McWilliams, K. A., Haaland, S., … Anderson, B. J. (2021). The Relationship Between Large Scale Thermospheric Density Enhancements and the Spatial Distribution of Poynting Flux. Journal of Geophysical Research: Space Physics, 126(5). https://doi.org/10.1029/2021JA029205

15-16 UT March 23, 2002

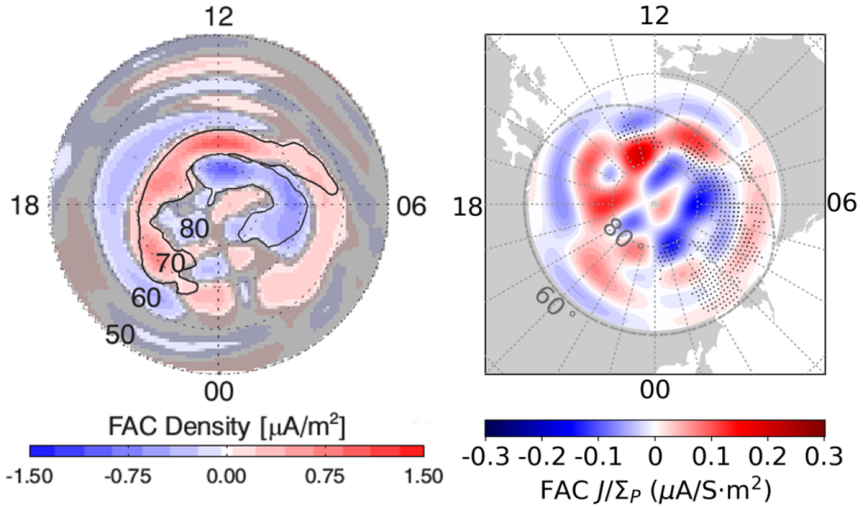

Wessel, M. R., SuperDARN electrostatic potential function estimation of field-aligned currents, 2017, MSc Thesis, University of Saskatchewan.

- SuperDARN can be used to estimate the *large-scale* field aligned currents via (Sofko et al., 1995):

$$\vec{J}_{\parallel} = \Sigma_P \vec{B} \cdot \nabla \times \vec{v} - \vec{E} \cdot \nabla \Sigma_P + \vec{B} \vec{v} \cdot \nabla \Sigma_H$$

Sofko, G. J., Greenwald, R., & Bristow, W. (1995). Direct determination of large-scale magnetospheric field-aligned currents with SuperDARN. Geophysical Research Letters, 22(15), 2041–2044. https://doi.org/10.1029/95GL01317

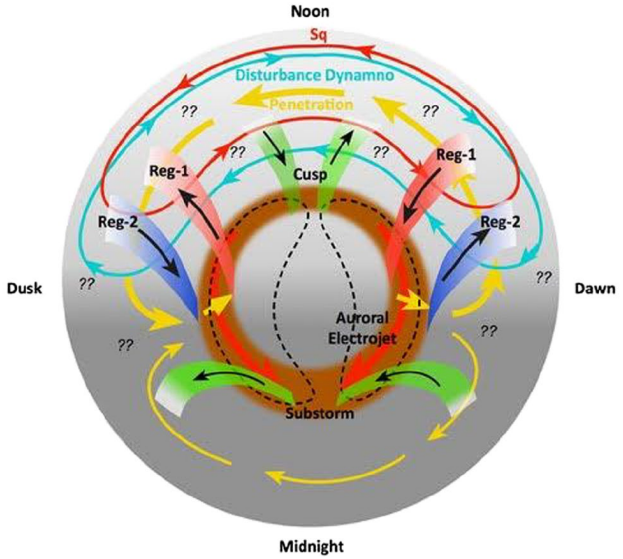

- *The connections to the magnetosphere and the corresponding response of the I-T are clearly influenced by electromagnetic energy flow, precipitating particles, and thermal plasma outflow. The challenge of incorporating these processes into computational models is matched by the acquisition of observations in the I-T that specify how these connecting properties vary in space and time within the I-T.*

Heelis, R. A., & Maute, A. (2020). Challenges to Understanding the Earth's Ionosphere and Thermosphere. Journal of Geophysical Research: Space Physics, 125(7), 1–44. https://doi.org/10.1029/2019JA027497

- Significant gaps remain in our understanding of how incident energy is deposited in altitude.
- The influence of the neutral winds has yet to be specified.
- Alfvénic heating is thought to play a significant role, but it is poorly characterized.
- Ground-based instruments are pivotal for science closure on these topics.

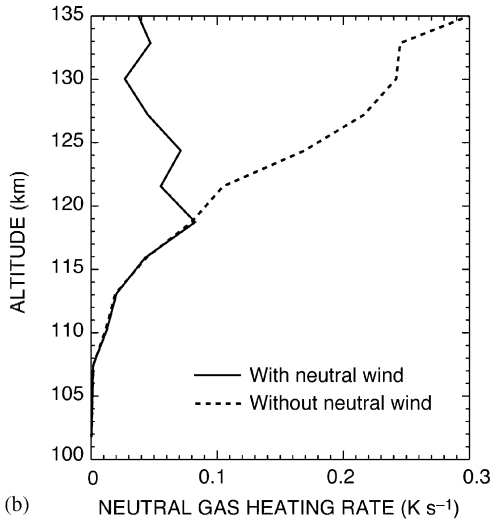

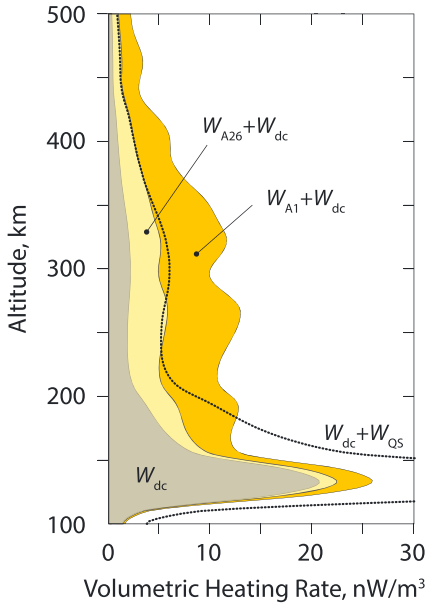

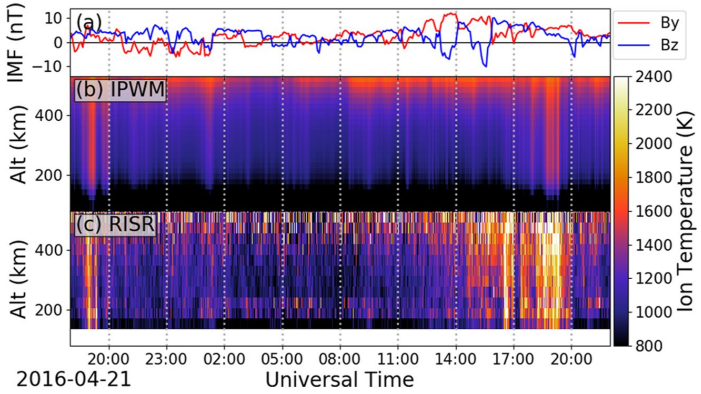

Thayer, J. P., & Semeter, J. (2004). The convergence of magnetospheric energy flux in the polar atmosphere. Journal of Atmospheric and Solar-Terrestrial Physics, 66(10), 807–824. https://doi.org/10.1016/j.jastp.2004.01.035

Lotko, W., & Zhang, B. (2018). Alfvénic Heating in the Cusp Ionosphere-Thermosphere. Journal of Geophysical Research: Space Physics, 123(12), 10,368-10,383. https://doi.org/10.1029/2018JA025990

Lamarche, L. J., Varney, R. H., & Reimer, A. S. (2021). Ion Heating in the Polar Cap Under Northwards IMF Bz. Journal of Geophysical Research: Space Physics, 126(11), 1–16. https://doi.org/10.1029/2021JA029155

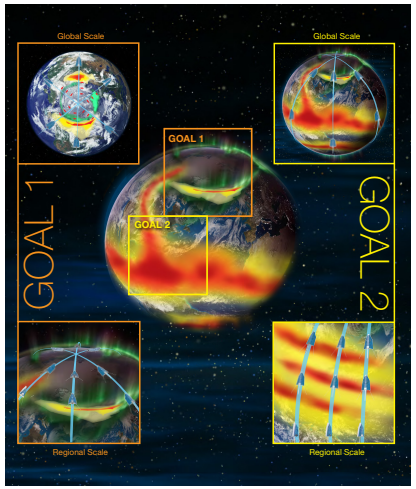

NASA STDT report for GDC, 2019

Mnemonic	Scale name	Scale size description	Spatial Scale[1], L	Temporal Scale[2], τ
LF	LOCAL-FAST	Local Scale, for rapid variations	300-2000 km	0.5 – 3 minutes
LS	LOCAL-SLOW	Local Scale, for slower variations	300-2000 km	>3 minutes
RF	REGIONAL-FAST	Regional Scale, for rapid variations	2000-4000 km	0.5 – 6 minutes
RS	REGIONAL-SLOW	Regional Scale, for slower variations	2000-4000 km	>6 minutes

Scale	Scale name	Scale size description	1st pair sep, LTAN[1]	2nd pair sep, LTAN[2]	Mean LTAN Sep.[3]	LTAN Span	Synch	Revisit Time
GS	GLOBAL-SLOW	Global Scale, for slower variations	2-4 hr	3-6 hr	<4 hr	>= 4.5 hr	<15 min.[4]	1 orbit period (~94 min)
GF	GLOBAL-FAST	Global Scale, for more rapid variations	3-6 hr	3-6 hr	<4 hr	>=3 hr	<15 min.[5]	15 min. to ½ orbit period (~47 min)

NASA GDC DRM, 2020

Primary	1	a	Thermal ion velocity, perpendicular to B (vector); *or* Electric field, perpendicular to B (vector)	± 5000 m/s *or* ± 250 mV/m	20 m/s *or* 0.5 mV/m
		b	Thermal ion velocity, parallel to B	± 2000 m/s	20 m/s
	2		Thermal plasma density	10^2 - 10^7 cm^{-3}	Larger of 100 cm^{-3} or 10%
	3		Thermal ion temperature	500 - 4000 K	Larger of 100 K or 10%
	4		Thermal ion composition (relative), by species	1 - 32 AMU	Larger of 100 cm^{-3} or 1%
	5	a	Neutral wind, horizontal (in-track)	± 1500 m/s	20 m/s
		b	Neutral wind, horizontal (cross-track)	± 1500 m/s	20 m/s
		c	Neutral wind, vertical (cross-track)	± 150 m/s	20 m/s
	6		Neutral gas number density	10^7 - 10^{10} cm^{-3}	10%
	7		Neutral gas temperature	400 - 2000 K	Larger of 50 K or 10%
	8		Neutral gas composition, by species	1 - 40 AMU	Larger of 10^4 cm^{-3} or 5%, per species
	9	a	Auroral electrons energy / pitch angle distribution (downgoing)	Energy range 0.05 - 20 keV, dE/E<20%, Pitch	
Secondary		b	Auroral electrons energy / pitch angle distribution (upgoing)	Energy range 0.05 - 20 keV, dE/E<20%, Pitch	
	10	a	Auroral ions energy / pitch angle distribution (downgoing)	No species discrimination required, Energy range;	
		b	Auroral ions energy / pitch angle distribution (upgoing)	Pitch Angle resolution 10°, Energy flux rang	
	11	a	Spatial structures, electric field (0.1-25 km)	500 mV/m	10.0%
		b	Spatial structures, thermal plasma density (0.1-25 km)	10^2 - 10^7 cm^{-3}	Larger of 100 cm^{-3} or 10%
	12		Thermal electron temperature	500 - 10000 K	Larger of 100 K or 10%
	13		Magnetic field perturbation (DC field, vector)	+/- 4000 nT	4 nT

NASA PEA-P for GDC, 2021

- GDC has the potential to significantly advance our understanding of MIT coupling at high-latitudes.
  - Contemporaneous measurements of the plasma, neutrals, and currents*, with 6 spacecraft will be unprecedented.
  - Alfvénic inputs into the topside ionosphere can be quantified.
  - Resolving conundrum such as the cusp neutral plasma density anomaly will be achievable.
  - Specification of mesoscale flow structures and associated chemistry in the polar-cap.
- GDC will provide the much needed global measurements of the MIT system and its dynamics for the modeling community (e.g., Heelis and Maute, 2021).
- However, GDC's impact will be diminished without sufficient ground-based facilities.
  - AMISRs, magnetometers, ASIs, etc..